PHYSICAL REVIEW D **88,** 074007 (2013)

Baryonia and near-threshold enhancements

Chengrong Deng,[1] Jialun Ping,[2,*] Youchang Yang,[3] and Fan Wang[4]
[1]*School of Mathematics and Physics, Chongqing Jiaotong University, Chongqing 400074, China*
[2]*Department of Physics, Nanjing Normal University, Nanjing 210097, China*
[3]*Department of Physics, Zunyi Normal College, Zunyi 563002, China*
[4]*Department of Physics, Nanjing University, Nanjing 210093, China*
(Received 28 June 2013; published 8 October 2013)

The baryon-antibaryon spectrum consisting of u, d, s, c, and b quarks is studied in the color flux-tube model with a multibody confinement interaction. Numerical results indicate that many low-spin ($S \leq 1$) baryon-antibaryon states can form compact bound states and are stable against decaying into a baryon and an antibaryon. They can be searched for in e^+e^- annihilation and charmonium or bottomonium decay if they really exist. Multibody confinement interaction as a binding mechanism plays an important role in the formation of the baryon-antibaryon bound states; chromomagnetic interaction also provides a strong attraction in many low-spin baryon-antibaryon states. The newly reported states, $X(1835)$, $X(2370)$, $Y(2175)$, $Y(4360)$, and $Y_b(10890)$, might be interpreted as $N\bar{N}$, $\Delta\bar{\Delta}$, $\Lambda\bar{\Lambda}$, $\Lambda_c\bar{\Lambda}_c$, and $\Lambda_b\bar{\Lambda}_b$ bound states, respectively.

DOI: 10.1103/PhysRevD.88.074007 PACS numbers: 12.39.Jh, 13.75.Cs, 14.40.Rt

I. INTRODUCTION

Baryonia research has a rather long history, which dates back to the 1940s. Fermi and Yang proposed that the π meson may be a composite particle, a nucleon-antinucleon ($N\bar{N}$) [1], in which a strong attractive force is assumed to bind them together, because the mass of a π meson is substantially smaller than twice the mass of a nucleon. Subsequently, Sakata extended Fermi and Yang's idea by introducing a strange baryon Λ and its antiparticle. The strange baryon Λ, proton p, neutron n, and their antiparticles were regarded as the fundamental building blocks to form other mesons and baryons, which is the well-known Fermi-Yang-Sakata (FYS) model [2]. The profound difficulty of the FYS model was that mesons and baryons other than p, n, and Λ would be formed by baryons and antibaryons, which is inconsistent with the observed properties of these hadrons. In 1964, the FYS model was therefore replaced by quark models, and the point of view that mesons might be $B\bar{B}$ states has been abandoned since then by most physicists. A new type of meson with a mass near the $B\bar{B}$ threshold and having specific decay properties called baryonia was proposed [3].

In recent years, many near-threshold enhancements have been observed. The $p\bar{p}$ enhancement is observed in the $J/\psi \to \gamma p\bar{p}$, $\psi' \to \pi^0 p\bar{p}$, $\eta p\bar{p}$, and $B^{\pm} \to p\bar{p}K^{\pm}$ processes [4]; the $\Lambda\bar{\Lambda}$ enhancement is observed in the $B^+ \to \Lambda\bar{\Lambda}K^+$ and $e^+e^- \to \Lambda\bar{\Lambda}$ processes [5]; the $\Lambda_c^+\Lambda_c^-$ enhancement is observed in the $e^+e^- \to \Lambda_c^+\Lambda_c^-$ process [6], and so on. Furthermore, other resonances called XYZ particles were also observed in experiments. It is hard to accommodate some of them, such as $X(3872)$ and $Y(4260)$, into $Q\bar{Q}$ quark models. Their extraordinary properties go beyond our anticipation based on the $Q\bar{Q}$ quark model; it is taken for granted that the heavy mesons can be well described with $Q\bar{Q}$ quark models. The appearance of XYZ particles inspired other interpretations rather than a $Q\bar{Q}$ configuration. An account of recent progresses and a rather complete list of references on XYZ particles can be found in the recent review, Ref. [7]. In addition to the compact tetraquark states, meson-meson molecular states, hybrid quarkonia, and orbital excited states of conventional mesons *et al.*, baryonia or hexaquark states $q^3\bar{q}^3$ are also proposed. The $p\bar{p}$ enhancement was interpreted as a baryonium $N\bar{N}$ with quantum numbers $J^{PC} = 0^{-+}$ in different models by many authors [8]. The states $Y(4260)$, $Y(4361)$, $Z^{\pm}(4430)$, and $Y(4664)$ were systematically embedded into an extended baryonium picture [9]. $Y(2175)$ was described as a bound state $\Lambda\bar{\Lambda}$ with quantum numbers $^{2S+1}L_J = {}^3S_1$ in the one-boson exchange (OBE) model [10].

Light nonstrange hexaquark systems $q^3\bar{q}^3$ were systematically studied in a color flux-tube model with a six-body confinement potential instead of an additive two-body interaction in our previous work, and it was found that some ground states are stable against disintegrating into a baryon and an antibaryon [11]. In the present work, the spectrum of the $B\bar{B}$ of the ground states consisting of u, d, s, c, and b quarks is studied in the color flux-tube model. This work is not only a natural extension of the previous work to understand the structure of the recently discovered resonances, but also provides a new insight to explore the baryonium states. Our model study shows that many low-spin $B\bar{B}$ states might be compact hexaquark states and stable against directly decaying into a baryon and an antibaryon. The multibody confinement interaction in the color flux-tube model plays an important role in the short-range domain, and the chromomagnetic interaction also

*Corresponding author.
jlping@njnu.edu.cn

 © 2013 American Physical Society

provides a strong attraction in the low-spin states. The dominant components of the new hadron states, $X(1835)$, $X(2370)$, $Y(2175)$, $Y(4260)$, and $Y_b(10890)$, may be interpreted as $N\bar{N}$, $\Delta\bar{\Delta}$, $\Lambda\bar{\Lambda}$, $\Lambda_c\bar{\Lambda}_c$, and $\Lambda_b\bar{\Lambda}_b$ bound states, respectively.

The paper is organized as follows: Sec. II is devoted to the description of the color flux-tube model and gives the Hamiltonian of baryons and hexaquark systems. A brief introduction to the construction of the wave functions of baryons and hexaquark systems is given in Sec. III. The numerical results and discussions are presented in Sec. IV. A brief summary is given in the last section.

II. COLOR FLUX-TUBE MODEL AND HAMILTONIAN

Quantum chromodynamics (QCD) is widely accepted as the fundamental theory to describe strong interacting systems and has been verified in high-momentum transfer processes. In the low-energy region, such as hadron spectroscopy and hadron-hadron interaction study, the *ab initio* calculation directly from QCD becomes very difficult due to the complication of nonperturbative nature. Although many nonperturbative methods have been developed, such as lattice QCD (LQCD), QCD sum rule, large-N_c expansion, chiral unitary theory, and so on, the QCD-inspired constituent quark model (CQM) is still a useful tool in obtaining physical insight for these complicated strong interacting systems. The CQM can offer the most complete description of hadron properties and is probably the most successful phenomenological model of hadron structure [12].

The CQM is formulated under the assumption that the hadrons are color-singlet nonrelativistic bound states of constituent quarks with phenomenological effective masses and interactions. The effective interactions include one-gluon exchange (OGE), OBE, and a confinement potential. The traditional CQM includes the typical Isgur-Karl model and chiral quark model [13,14], in which the confinement potential can be phenomenologically described as the sum of two-body interactions proportional to the color charges and r_{ij}^k,

$$V^C = -a_c \sum_{i>j}^{n} \boldsymbol{\lambda}_i \cdot \boldsymbol{\lambda}_j r_{ij}^k, \tag{1}$$

where r_{ij} is the distance between two interacting quarks q_i and q_j, and k usually takes 1 or 2. The traditional models can describe the properties of ordinary hadrons (q^3 and $q\bar{q}$) well. However, the traditional models lead to power-law van der Waals forces between color-singlet hadrons and the anticonfinement in a color-symmetrical quark or antiquark pair. The problems are related to the fact that the traditional CQM does not respect local color-gauge invariance.

The color flux-tube structures of ordinary hadrons are unique and trivial; important low-energy QCD information may be absent in the descriptions of these objects, such as the interaction of a quark (antiquark) pair in color-symmetrical 6 ($\bar{6}$) representation. Multiquark systems, if they really exist, have various color flux-tube structures in the intermediate- and short-distance domains, which may contain abundant low-energy QCD information and affect the properties of multiquark systems [15–19]. The mixing effect of the color flux-tube structures can provide the intermediate-range attractive force coming from the σ meson or $\pi\pi$ exchange [20]. The various color flux-tube structures of multiquark systems are hard to describe using the two-body confinement potential in the traditional CQM.

LQCD calculations of ordinary hadrons, tetraquark and pentaquark states reveal various color flux-tube structures [21]. Within the color flux-tube picture, the confinement potential of multiquark states is a multibody interaction and can be simulated by a potential which is proportional to the minimum of the total length of all color flux tubes which connect the quarks (antiquarks) to form the multiquark system [21]. Based on the traditional CQM and the LQCD picture, the color flux-tube model has been developed to study multiquark systems, in which a multibody confinement interaction is employed, and a sum of the square of the length of flux tubes rather than a linear relationship is assumed to simplify the calculation [15–19]. The approximation is justified for the following two reasons: One is that the spatial variations in the separation of the quarks (lengths of the flux tubes) in different hadrons do not differ significantly, so the difference between the two functional forms is small and can be absorbed in the adjustable parameter, the stiffness. The other is that we are using a nonrelativistic dynamics in the study. As was shown long ago [22], an interaction energy that varies linearly with separation between fermions in a relativistic first-order differential dynamics has a wide region in which a harmonic approximation is valid for the second-order (Feynman-Gell-Mann) reduction of the equations of motion. The comparative studies also indicated that the difference between the two types of confinement potentials is very small [18,19].

In the color flux-tube picture, it is assumed that the color-electric flux is confined to narrow, flux-tube-like tubes joining quarks and antiquarks. A color flux tube starts from each quark and ends at an antiquark or a Y-shaped junction, where three color flux tubes are either annihilated or created [23]. The Y-shaped color flux-tube structure, the LQCD picture of a baryon [24], is shown in Fig. 1, in which $\mathbf{r}_i$ represents the spatial position of the ith quark, denoted by a black dot, and $\mathbf{y}_0$ denotes a junction where three color flux tubes meet. The three-body quadratic confinement potential can be written as

$$V^C(3) = K((\mathbf{r}_1 - \mathbf{y}_0)^2 + (\mathbf{r}_2 - \mathbf{y}_0)^2 + (\mathbf{r}_3 - \mathbf{y}_0)^2). \tag{2}$$

The position of the junction $\mathbf{y}_0$ can be fixed by minimizing the energy of baryons, and then we get

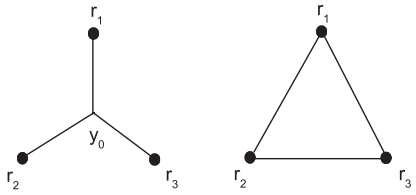

FIG. 1. Three-body (left) and two-body (right) confinement potential.

$$\mathbf{y}_0 = \frac{\mathbf{r}_1 + \mathbf{r}_2 + \mathbf{r}_3}{3}. \quad (3)$$

The minimum of the confinement potential has, therefore, the following forms:

$$V^C_{\min}(3) = K\left(\left(\frac{\mathbf{r}_1 - \mathbf{r}_2}{\sqrt{2}}\right)^2 + \left(\frac{2\mathbf{r}_3 - \mathbf{r}_1 - \mathbf{r}_2}{\sqrt{6}}\right)^2\right). \quad (4)$$

The above equation can also be expressed as the sum of three pairs of two-body interactions,

$$V^C_{\min}(3) = \frac{K}{3}((\mathbf{r}_1 - \mathbf{r}_2)^2 + (\mathbf{r}_2 - \mathbf{r}_3)^2 + (\mathbf{r}_1 - \mathbf{r}_3)^2). \quad (5)$$

It can be seen that the three-body quadratic confinement potential of a baryon is totally equivalent to the sum of the two-body one—see the Δ-shaped structure in Fig. 1—although the equivalence is only approximately valid for the linear confinement potential.

The color flux-tube structures of a multiquark system with $N + 1$ particles can be generated by replacing a quark or an antiquark in an N-particle state with a Y-shaped junction and two antiquarks or two quarks. A hexaquark system $q^3\bar{q}^3$ has at least four possible color flux-tube structures listed in Fig. 2, in which a black dot denotes a quark and a hollow dot denotes an antiquark. A thin line connecting a quark and a junction represents a fundamental color flux tube, namely a color triplet. A thick line connecting two junctions represents a compound color flux tube, namely a color sextet, octet, or others. The different dimensional color flux tubes may have different stiffness, which will be discussed in the latter part of this section. The numbers (d_{ij}) on the color flux tubes represent the dimensions of the corresponding color flux tube. The dimension d_{23} in the structures (b) and (c) may be, respectively, (8, 10) and (3, $\bar{6}$, 15). The dimensions $(d_{16}, d_{63}, d_{35}, d_{52}, d_{24}, d_{41})$ in the structure (d) at least may be $(\bar{3}, 3, \bar{3}, 3, \bar{3}, 3)$ and (3, 8, 3, 8, 3, 8). The arrows in the color flux tubes represent the color coupling direction. Both the overall color-singlet nature of a multiquark system and the $SU(3)$ color coupling rule at each junction must be satisfied.

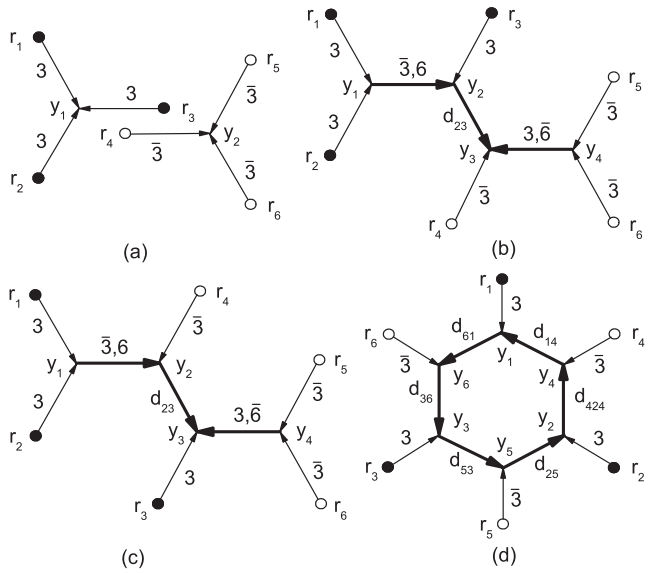

FIG. 2. Four possible color flux-tube structures of a hexaquark system $q^3\bar{q}^3$.

A color flux-tube structure specifies the corresponding color configuration (how the colors of quarks and antiquarks are coupled to form an overall color singlet). In general, each color flux-tube structure has various color configurations according to quark correlation. Quark correlation plays an important role in a multiquark system [25]. A hexaquark system $q^3\bar{q}^3$ has many clustering configurations, such as $[q^3][\bar{q}^3]$, $[q\bar{q}^2][q^2\bar{q}]$, $[q][q^2\bar{q}^3]$, $[q^2][q\bar{q}^3]$, $[\bar{q}][\bar{q}^2q^3]$, $[\bar{q}^2][\bar{q}q^3]$, $[q\bar{q}][\bar{q}^2q^2]$, and so on. In the present work, only two symmetrical configurations under quark-antiquark exchange, $[q^3][\bar{q}^3]$ and $[q\bar{q}^2][q^2\bar{q}]$, are considered. In this way, the structure (a) may be a $B\bar{B}$ molecule state: $[q^3]_1[\bar{q}^3]_1$. The structure (b) may be called a hidden color baryon-antibaryon state, and it has two color configurations: $[[q^3]_{10}[\bar{q}^3]_{\bar{10}}]_1$ and $[[q^3]_8[\bar{q}^3]_8]_1$. The structure (c) may be called a diquark-antidiquark state and has four possible color configurations: $[[[q^2]_{\bar{3}}\bar{q}]_3 \times [[\bar{q}^2]_3q]_{\bar{3}}]_1$, $[[[q^2]_{\bar{3}}\bar{q}]_{\bar{6}}[[\bar{q}^2]_3q]_6]_1$, $[[[q^2]_6\bar{q}]_3[[\bar{q}^2]_{\bar{6}}q]_{\bar{3}}]_1$, and $[[[q^2]_6\bar{q}]_{15}[[\bar{q}^2]_{\bar{6}}q]_{\bar{15}}]_1$. The last of these is very similar to a chemical benzene, and it is therefore called QCD benzene. The color configuration of this structure is hard to describe only using quark degrees of freedom in the framework of the quark models, which is worthy of study in the future. A hexaquark state q^6 with this structure was investigated in our previous work [18]. Of course, the color flux-tube structures should include a three-color-singlet meson configuration: $[q\bar{q}]_1[q\bar{q}]_1[q\bar{q}]_1$, which must be taken into account in the decay of a $q^3\bar{q}^3$ system into three color-singlet mesons. This task, too, is left for future study. The color flux tube in hadrons should be very similar to the chemical bond in organic compounds. The same molecular constituents may have different chemical bond structures; these are called isomeric compounds. Therefore, multiquark systems with the same quark content but different flux-tube structures are similarly called QCD isomeric compounds.

In general, a hexaquark system $q^3\bar{q}^3$ should be the mixture of all possible color flux-tube structures. In order

to avoid a too-complicated calculation in the present work, only the structures (a) and (b) in Fig. 2 are considered. Within the color flux-tube model, the confinement potential for the structure (a) can be written as

$$V^a_{\min}(6) = K\Big(\Big(\frac{\mathbf{r}_1-\mathbf{r}_2}{\sqrt{2}}\Big)^2 + \Big(\frac{2\mathbf{r}_3-\mathbf{r}_1-\mathbf{r}_2}{\sqrt{6}}\Big)^2 + \Big(\frac{\mathbf{r}_4-\mathbf{r}_5}{\sqrt{2}}\Big)^2 + \Big(\frac{2\mathbf{r}_6-\mathbf{r}_4-\mathbf{r}_5}{\sqrt{6}}\Big)^2\Big). \quad (6)$$

The confinement potential for the structure (b) has the following form:

$$V^b(6) = K((\mathbf{r}_1-\mathbf{y}_1)^2 + (\mathbf{r}_2-\mathbf{y}_1)^2 + (\mathbf{r}_3-\mathbf{y}_2)^2 + (\mathbf{r}_4-\mathbf{y}_3)^2 + (\mathbf{r}_5-\mathbf{y}_4)^2 + (\mathbf{r}_6-\mathbf{y}_4)^2 + \kappa_{d_{12}}(\mathbf{y}_1-\mathbf{y}_2)^2 + \kappa_{d_{23}}(\mathbf{y}_2-\mathbf{y}_3)^2 + \kappa_{d_{34}}(\mathbf{y}_3-\mathbf{y}_4)^2). \quad (7)$$

In the above equations, K is the stiffness of an elementary color flux tube, while $K\kappa_{d_{ij}}$ is the stiffness of other compound color flux tubes. The relative stiffness $\kappa_{d_{ij}}$ depends on the dimension, d_{ij}, of the compound color flux tube [26]

$$\kappa_{d_{ij}} = \frac{C_{d_{ij}}}{C_3}, \quad (8)$$

where $C_{d_{ij}}$ is the eigenvalue of the Casimir operator associated with the $SU(3)$ color representation d_{ij} on either end of the color flux tube, such as $C_3 = \frac{4}{3}$, $C_6 = \frac{10}{3}$, or $C_8 = 3$. For the sake of simplicity, the arithmetic average κ_d for all relative stiffness $\kappa_{d_{ij}}$ in each structure is used in numerical calculations, namely

$$\kappa_d = \frac{\kappa_{d_{12}} + \kappa_{d_{23}} + \kappa_{d_{34}}}{3}. \quad (9)$$

For given quark (antiquark) positions $\mathbf{r}_i$, those junctions $\mathbf{y}_i$ can be obtained by minimizing the confinement potential. By introducing the following set of canonical coordinates $\mathbf{R}_i$,

$$\mathbf{R}_1 = \frac{1}{\sqrt{2}}(\mathbf{r}_1-\mathbf{r}_2), \qquad \mathbf{R}_2 = \frac{1}{\sqrt{2}}(\mathbf{r}_5-\mathbf{r}_6),$$
$$\mathbf{R}_3 = \frac{1}{\sqrt{12}}(\mathbf{r}_1+\mathbf{r}_2-2\mathbf{r}_3-2\mathbf{r}_4+\mathbf{r}_5+\mathbf{r}_6),$$
$$\mathbf{R}_4 = \frac{1}{\sqrt{33+5\sqrt{33}}}(\mathbf{r}_1+\mathbf{r}_2-w_1\mathbf{r}_3+w_1\mathbf{r}_4-\mathbf{r}_5-\mathbf{r}_6),$$
$$\mathbf{R}_5 = \frac{1}{\sqrt{33-5\sqrt{33}}}(\mathbf{r}_1+\mathbf{r}_2+w_2\mathbf{r}_3-w_2\mathbf{r}_4-\mathbf{r}_5-\mathbf{r}_6),$$
$$\mathbf{R}_6 = \frac{1}{\sqrt{6}}(\mathbf{r}_1+\mathbf{r}_2+\mathbf{r}_3+\mathbf{r}_4+\mathbf{r}_5+\mathbf{r}_6), \quad (10)$$

the minimum of the confinement potential takes the following form:

$$V^b_{\min}(6) = K\Big(\mathbf{R}_1^2+\mathbf{R}_2^2+\frac{3\kappa_d}{2+3\kappa_d}\mathbf{R}_3^2 + \frac{2\kappa_d(\kappa_d+w_3)}{2\kappa_d^2+7\kappa_d+2}\mathbf{R}_4^2 + \frac{2\kappa_d(\kappa_d+w_4)}{2\kappa_d^2+7\kappa_d+2}\mathbf{R}_5^2\Big), \quad (11)$$

where $w_1 = \frac{\sqrt{33}+5}{2}$, $w_2 = \frac{\sqrt{33}-5}{2}$, $w_3 = \frac{7+\sqrt{33}}{4}$, and $w_4 = \frac{7-\sqrt{33}}{4}$. Clearly this confinement potential is a multibody interaction rather than the sum of a two-body one. When two clusters q^3 and $\bar{q}^3$ separate in large distances, a baryon and an antibaryon should be a dominant component of the system, because other hidden color flux-tube structures are suppressed due to the color confinement. With the separation reducing, a hadronic molecule state may be formed if the attractive force between a baryon and an antibaryon is strong enough. When they are close enough to be within the range of confinement (about 1 fm), all possible flux-tube structures may appear due to the excitation and rearrangement of color flux tubes. In this case, the confinement potential of the system should at least be taken to be the minimum of the two flux-tube structures. It therefore reads

$$V^C_{\min}(6) = \min(V^a_{\min}, V^b_{\min}). \quad (12)$$

OGE and (or) OBE are important and responsible for the mass splitting in the ordinary hadron spectra. The model with OGE and the model with OGE plus OBE can both describe the ground states of baryons well; the differences between the two models appear in the description of excited baryons [27]. The study on the ground states of nonstrange hexaquark systems $q^3\bar{q}^3$ indicates that the difference between the two models is small [17]; therefore, only OGE is taken into account in the present work. The complete Hamiltonian used here is listed as the following:

$$H_n = \sum_{i=1}^{n}\Big(m_i + \frac{\mathbf{p}_i^2}{2m_i}\Big) - T_C + \sum_{i>j}^{n} V^G_{ij} + V^C_{\min}(n), \quad (13)$$

$$V^G_{ij} = \frac{1}{4}\alpha_s\boldsymbol{\lambda}_i\cdot\boldsymbol{\lambda}_j\Big(\frac{1}{r_{ij}} - \frac{2\pi}{3}\delta(\mathbf{r}_{ij})\frac{\boldsymbol{\sigma}_i\cdot\boldsymbol{\sigma}_j}{m_i m_j}\Big). \quad (14)$$

The tensor force and spin-orbit force between quarks are omitted in the model, because our primary interest is in the lowest energies, and their contributions to the ground states are small or zero. In the above expression of H_n, $n = 3$ or $n = 6$, T_C is the center-of-mass kinetic energy, m_i and $\mathbf{p}_i$ are the mass and momentum of the ith quark, and $\boldsymbol{\lambda}$ and $\boldsymbol{\sigma}$ are the $SU(3)$ Gellman and $SU(2)$ Pauli matrices, respectively. Note that $\boldsymbol{\lambda} \to -\boldsymbol{\lambda}^*$ for the antiquark; all other symbols have their usual meanings. An effective scale-dependent strong coupling constant is used here [28],

$$\alpha_s(\mu) = \frac{\alpha_0}{\ln\Big(\frac{\mu^2+\mu_0^2}{\Lambda_0^2}\Big)}, \quad (15)$$

where μ is the reduced mass of two interactional quarks q_i and q_j, namely $\mu = \frac{m_i m_j}{m_i + m_j}$. Λ_0, α_0, and μ_0 are model parameters. The δ function, arising as a consequence of the nonrelativistic reduction of the OGE diagram between pointlike particles, has to be regularized in order to perform numerical calculations. It reads [29]

$$\delta(r_{ij}) = \frac{1}{\beta^3 \pi^{\frac{3}{2}}} e^{-\frac{r_{ij}^2}{\beta^2}}, \tag{16}$$

where β is a model parameter which is determined by fitting the experiment data in Sec. IV.

As far as a baryon is concerned, the color flux-tube model reduces to the traditional quark model. However, if it is applied to multiquark systems, the confinement potential is a multibody interaction instead of a color-dependent two-body one used in traditional quark models [15–19]. In fact, the color flux-tube model based on traditional quark models and the LQCD picture merely modifies the two-body confinement potential to describe possible multiquark states with multibody confinement potential.

III. WAVE FUNCTIONS AND THE GAUSSIAN EXPANSION METHOD

The total wave function of baryons can be written as the direct products of color, isospin, spin, and spatial terms,

$$\Phi^{q^3}_{IM_I JM_J}(\mathbf{R}, \mathbf{r}) = \chi_c [\Psi^G_{L_T M_T}(\mathbf{R}, \mathbf{r}) \eta_{IM_I SM_S}]_{IM_I JM_J}, \tag{17}$$

in which $[\cdots]_{IM_I JM_J}$ means coupling the spin S and total orbital angular momentum L_T with Clebsch-Gordan coefficients. The color-part wave function χ_c is antisymmetrical because of the color-singlet requirement. Only u and d quarks are regarded as identical particles; the $SU_{sf}(4) \supset SU_s(2) \otimes SU_f(2)$ symmetry is therefore used in the spin-flavor wave function $\eta_{IM_I SM_S}$. The spatial wave functions of identical particles are assumed to be symmetrical because we are interested in the ground states. We can define Jacobi coordinates $\mathbf{r}_{ij}$ and $\mathbf{R}_k$ for the cyclic permutations of (1, 2, 3):

$$\mathbf{r}_{ij} = \mathbf{r}_i - \mathbf{r}_j, \qquad \mathbf{R}_k = \mathbf{r}_k - \frac{m_i \mathbf{r}_i + m_j \mathbf{r}_j}{m_i + m_j}. \tag{18}$$

Within the framework of the Gaussian expansion method (GEM) [30], the total spatial symmetrical wave functions of baryons with three identical particles, such as N, Δ, and Ω, can be expressed as

$$\Psi_{L_T M_T}(\mathbf{R}, \mathbf{r}) = \sum_{i,j,k=1}^{3} [\phi_{lm}(\mathbf{r}_{ij}) \phi_{LM}(\mathbf{R}_k)]_{L_T M_T}. \tag{19}$$

For baryons with only two identical particles, such as Λ and Σ, the spatial wave function has the following form:

$$\Psi_{L_T M_T}(\mathbf{R}, \mathbf{r}) = [\phi_{lm}(\mathbf{r}_{ij}) \phi_{LM}(\mathbf{R}_k)]_{L_T M_T}, \tag{20}$$

in which quarks q_i and q_j are identical particles. The spatial wave function of baryons with three different quarks is the same as Eq. (20), in which the quark q_k is the heaviest one.

The relative-motion wave functions $\phi_{lm}(\mathbf{r}_{ij})$ and $\phi_{LM}(\mathbf{R}_k)$ are the superpositions of Gaussian basis functions with different sizes,

$$\phi_{lm}(\mathbf{r}_{ij}) = \sum_{n=1}^{n_{\max}} c_n N_{nl} r_{ij}^l e^{-\nu_n r_{ij}^2} Y_{lm}(\hat{\mathbf{r}}_{ij}), \tag{21}$$

$$\psi_{LM}(\mathbf{R}_k) = \sum_{N=1}^{N_{\max}} c_N N_{NL} R_k^L e^{-\nu_N R_k^2} Y_{LM}(\hat{\mathbf{R}}_k), \tag{22}$$

where N_{nl} and N_{NL} are normalization constants. Gaussian size parameters ν_n and ν_N are taken as geometric progression:

$$r_n = r_1 a^{n-1}, \qquad \nu_n = \frac{1}{r_n^2}, \qquad a = \left(\frac{r_{n_{\max}}}{r_1}\right)^{\frac{1}{n_{\max}-1}}, \tag{23}$$

$$R_N = R_1 A^{N-1}, \qquad \nu_N = \frac{1}{R_N^2}, \qquad A = \left(\frac{R_{N_{\max}}}{R_1}\right)^{\frac{1}{N_{\max}-1}}. \tag{24}$$

The numbers n and l (N and L) specify, respectively, the radial and angular momenta excitations with respect to the Jacobi coordinate $\mathbf{r}$ ($\mathbf{R}$). The angular momenta l and L are coupled to the total orbit angular momentum L_T.

With regard to a hexaquark system $q^3\bar{q}^3$, the Jacobi coordinates are shown in Fig. 3 and can be expressed as

$$\begin{aligned} \mathbf{r}_{ij} &= \mathbf{r}_i - \mathbf{r}_j, \qquad \mathbf{R}_k = \mathbf{r}_k - \frac{m_i \mathbf{r}_i + m_j \mathbf{r}_j}{m_i + m_j}, \\ \mathbf{r}_{lm} &= \mathbf{r}_l - \mathbf{r}_m, \qquad \mathbf{R}_n = \mathbf{r}_n - \frac{m_l \mathbf{r}_l + m_m \mathbf{r}_m}{m_l + m_m}, \\ \mathbf{X} &= \frac{m_i \mathbf{r}_i + m_j \mathbf{r}_j + m_k \mathbf{r}_k}{m_i + m_j + m_k} - \frac{m_l \mathbf{r}_l + m_m \mathbf{r}_m + m_n \mathbf{r}_n}{m_l + m_m + m_n}. \end{aligned} \tag{25}$$

The model wave function with fixed quantum numbers I and J can be expressed as

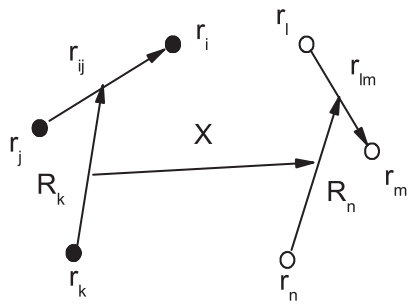

FIG. 3. Jacobi ordinates for a hexaquark system $q^3\bar{q}^3$.

$$\Psi_{IJ}^{[q^3][\bar{q}^3]} = \sum_{\xi} c_{\xi}[[\Phi_{c_1 I_1 J_1}^{q^3} \Phi_{c_2 I_2 J_2}^{\bar{q}^3}]_{\xi} F(\mathbf{X})]_{IJ}. \quad (26)$$

$\Phi_{c_1 I_1 J_1}^{q^3}$ and $\Phi_{c_2 I_2 J_2}^{\bar{q}^3}$ are the cluster wave functions of the colorful or color-singlet baryon q^3 and antibaryon $\bar{q}^3$, respectively, in which the spatial functions are the same as those shown before for baryons, and $[\cdots]_{\xi}$ represents all the needed coupling: color, isospin, and spin. All the possible channels are taken into account in our multichannel coupling calculation. $F(\mathbf{X})$ is the relative orbital wave function between q^3 and $\bar{q}^3$ clusters; it is also expanded by Gaussian basis functions with different sizes,

$$F(\mathbf{X}) = \sum_{N'=1}^{N'_{\max}} c_{N'} N_{N'L'} X^{L'} e^{-\nu_{N'} X^2} Y_{L'M'}(\hat{\mathbf{X}}). \quad (27)$$

The Gaussian size parameter $\nu_{N'}$ is taken to have the same form as ν_n or ν_N.

IV. NUMERICAL RESULTS AND DISCUSSIONS

The mass spectrum of the ground states of baryons can be obtained by solving the three-body Schrödinger equation

$$(H_3 - E_{IJ})\Phi_{IM_I JM_J}^{q^3}(\mathbf{R}, \mathbf{r}) = 0 \quad (28)$$

with the Rayleigh-Ritz variational principle. The converged results are arrived at by setting $r_1 = R_1 = 0.3$ fm, $r_{n_{\max}} = R_{n_{\max}} = 2.0$ fm, and $n_{\max} = N_{\max} = 5$. The model parameters are fixed by fitting the experimental data, with the exception that the parameters Λ_0 and μ_0 are taken from the Ref. [28]: $\Lambda_0 = 0.187$ fm and $\mu_0 = 0.113$ fm. The values of the model parameters and the masses of the ground baryon are listed in Tables I and II, respectively. In general, the model can describe the baryon spectrum well.

The color flux-tube model with the model parameters listed in Table I is used to study the hexaquark systems $q^3\bar{q}^3$. It should be emphasized that no new parameter is introduced in the calculation of the hexaquark systems $q^3\bar{q}^3$. The mass spectrum of the hexaquark systems $q^3\bar{q}^3$ can be obtained by solving the six-body Schrödinger equation

$$(H_6 - E_{IJ})\Psi_{IJ}^{[q^3][\bar{q}^3]} = 0. \quad (29)$$

The converged numerical results can be obtained by setting $n_{\max} = 5$, $N_{\max} = 5$, and $N'_{\max} = 5$. The minimum and maximum ranges of the bases are 0.3 and 2.0 fm, respectively, for coordinates $\mathbf{r}$, $\mathbf{R}$, and $\mathbf{X}$.

TABLE I. Adjustable model parameters.

Parameters:	m_{ud}	m_s	m_c	m_b	α_0	K	β
Units:	MeV	MeV	MeV	MeV	$\cdots$	MeV fm^{-2}	fm
Values:	313	545	1800	5140	5.41	400	0.47

TABLE II. The masses of the ground states of baryons, units in MeV, in which n stands for a u or d quark.

Baryons	Flavor	IJ^P	Calculated	Experimental
N	nnn	$\frac{1}{2}\frac{1}{2}^+$	939	939
Λ	nns	$0\frac{1}{2}^+$	1108	1116
Σ	nns	$1\frac{1}{2}^+$	1213	1195
Ξ	nss	$\frac{1}{2}\frac{1}{2}^+$	1350	1315
Δ	nnn	$\frac{3}{2}\frac{3}{2}^+$	1232	1232
Σ^*	nns	$1\frac{3}{2}^+$	1382	1385
Ξ^*	nss	$\frac{1}{2}\frac{3}{2}^+$	1528	1530
Ω^-	sss	$0\frac{3}{2}^+$	1675	1672
Λ_c^+	nnc	$0\frac{1}{2}^+$	2287	2285
Σ_c	nnc	$1\frac{1}{2}^+$	2480	2455
Σ_c^*	nnc	$1\frac{3}{2}^+$	2533	2520
Ξ_c	nsc	$\frac{1}{2}\frac{1}{2}^+$	2620	2466
Ξ_c^*	nsc	$\frac{1}{2}\frac{3}{2}^+$	2670	2645
Ω_c^0	ssc	$0\frac{1}{2}^+$	2790	2695
Ω_c^{0*}	ssc	$0\frac{3}{2}^+$	2819	2766
Λ_b^0	nnb	$0\frac{1}{2}^+$	5600	5620
Σ_b	nnb	$1\frac{1}{2}^+$	5816	5808
Σ_b^*	nnb	$1\frac{3}{2}^+$	5836	5830
Ξ_b	nsb	$\frac{1}{2}\frac{1}{2}^+$	5948	5790
Ξ_b^*	nsb	$\frac{1}{2}\frac{3}{2}^+$	5966	$\cdots$
Ω_b^-	ssb	$0\frac{1}{2}^+$	6107	6071

The binding energies, $\Delta E_J = E_{IJ} - 2M_B$, of the ground states of the hexaquark systems $q^3\bar{q}^3$ are listed in Table III. It can be seen that the energies of many low-spin ($S \leq 1$) states lie below the threshold $2M_B$; the ground states are therefore stable against dissociation into a baryon and an antibaryon, while they can decay into three color-singlet mesons. None of the high-spin ($S \geq 2$) states lie below the corresponding threshold. To check the rationality of the various color structures used, the spatial configurations of the bound states are calculated by using the wave functions obtained in solving the Schrödinger equation. The rms for $\mathbf{r}$, $\mathbf{R}$, and $\mathbf{X}$ of all possible bound states $q^3\bar{q}^3$ with $J^{PC} = 0^{-+}$ and 1^{--} are listed in Table IV; it can be seen that they are smaller than 1 fm in the color flux-tube model. Numerical results in Tables III and IV indicate a tendency that the heavier the states are, the deeper the binding and the smaller the size. Taking the group $\Lambda\bar{\Lambda} - \Lambda_c\bar{\Lambda}_c - \Lambda_b\bar{\Lambda}_b$ as an example, the binding energies are, respectively, -80 MeV, -244 MeV, and -363 MeV. The distances between two clusters q^3 and $\bar{q}^3$ $\langle \mathbf{X}^2 \rangle^{\frac{1}{2}}$ are, respectively, 0.49, 0.39, and 0.38 fm. The same tendency appears in $\Sigma\bar{\Sigma} - \Sigma_c\bar{\Sigma}_c - \Sigma_b\bar{\Sigma}_b$ and $\Sigma^*\bar{\Sigma}^* - \Sigma_c^*\bar{\Sigma}_c^* - \Sigma_b^*\bar{\Sigma}_b^*$ systems and other groups. The reason

TABLE III. The binding energies of the ground states of $B\bar{B}$ states with quantum numbers J^{PC}, units in MeV, where "$\cdots$" means that the corresponding state does not exist. For the states with the lowest energies, all the orbital angular momenta are set to zero; therefore, the parity of the $B\bar{B}$ states is negative and the C parity is $(-1)^S$, because the baryonia are pure neutral systems.

States	0^{-+}	1^{--}	2^{-+}	3^{--}
$N\bar{N}$	-46	0	$\cdots$	$\cdots$
$\Lambda\bar{\Lambda}$	-80	-46	0	0
$\Sigma\bar{\Sigma}$	-10	0	$\cdots$	$\cdots$
$\Xi\bar{\Xi}$	-8	0	$\cdots$	$\cdots$
$\Delta\bar{\Delta}$	-80	0	0	0
$\Sigma^*\bar{\Sigma}^*$	-20	0	0	0
$\Xi^*\bar{\Xi}^*$	-105	-47	0	0
$\Omega^-\Omega^+$	-8	0	0	0
$\Lambda_c^+\Lambda_c^-$	-244	-232	$\cdots$	$\cdots$
$\Sigma_c\bar{\Sigma}_c$	-144	-132	$\cdots$	$\cdots$
$\Sigma_c^*\bar{\Sigma}_c^*$	-34	0	0	0
$\Xi_c\bar{\Xi}_c$	-207	0	$\cdots$	$\cdots$
$\Xi_c^*\bar{\Xi}_c^*$	-168	-98	0	0
$\Omega_c^0\bar{\Omega}_c^0$	0	0	$\cdots$	$\cdots$
$\Omega_c^{0*}\bar{\Omega}_c^{0*}$	0	0	0	0
$\Lambda_b^+\Lambda_b^-$	-363	-360	$\cdots$	$\cdots$
$\Sigma_b\bar{\Sigma}_b$	-278	-277	$\cdots$	$\cdots$
$\Sigma_b^*\bar{\Sigma}_b^*$	-58	-10	0	0
$\Xi_b\bar{\Xi}_b$	-304	-44	$\cdots$	$\cdots$
$\Xi_b^*\bar{\Xi}_b^*$	-266	-200	$\cdots$	$\cdots$
$\Omega_b^-\Omega_b^+$	0	0	$\cdots$	$\cdots$

for this tendency is that the large mass of heavy quarks depresses the motion domain and reduces the kinetic energy. The results agree with the tetraquark state calculations [31].

The sizes of all possible bound states in Table IV show that the dominant component is not a loose $B\bar{B}$ molecule state but a compact hexaquark state, which is formed by means of the multibody confinement potential originating from the color flux-tube picture, so the introduction of hidden color configuration is reasonable. Compared with the early baryonia calculations in the traditional quark models [32,33], where no nonstrange bound state was found, the multibody confinement interaction used in our model can globally give more attraction than the additive two-body one proportional to the color factor in the traditional quark models. Furthermore, the anticonfinement between a color-symmetrical quark or antiquark pair does not appear in the multibody confinement potential, because no color charge appears [15–17]. The similar string model with a multibody confinement potential was applied to study the stabilities of tetraquark, pentaquark, and hexaquark states, and it was suggested that many compact multiquark states could exist [34].

TABLE IV. The rms for $\mathbf{r}$, $\mathbf{R}$, and $\mathbf{X}$ of all possible $B\bar{B}$ bound states listed in Table III, units in fm.

J^{PC}	0^{-+}			1^{--}		
Rms	$\langle\mathbf{r}^2\rangle^{\frac{1}{2}}$	$\langle\mathbf{R}^2\rangle^{\frac{1}{2}}$	$\langle\mathbf{X}^2\rangle^{\frac{1}{2}}$	$\langle\mathbf{r}^2\rangle^{\frac{1}{2}}$	$\langle\mathbf{R}^2\rangle^{\frac{1}{2}}$	$\langle\mathbf{X}^2\rangle^{\frac{1}{2}}$
$N\bar{N}$	0.81	0.71	0.68	$\cdots$	$\cdots$	$\cdots$
$\Lambda\bar{\Lambda}$	0.76	0.66	0.49	0.77	0.69	0.54
$\Sigma\bar{\Sigma}$	0.86	0.67	0.87	$\cdots$	$\cdots$	$\cdots$
$\Xi\bar{\Xi}$	0.72	0.69	0.73	$\cdots$	$\cdots$	$\cdots$
$\Delta\bar{\Delta}$	0.93	0.82	0.62	$\cdots$	$\cdots$	$\cdots$
$\Sigma^*\bar{\Sigma}^*$	0.89	0.78	0.51	$\cdots$	$\cdots$	$\cdots$
$\Xi^*\bar{\Xi}^*$	0.75	0.77	0.47	0.75	0.80	0.48
$\Omega^-\Omega^+$	0.75	0.70	0.45	$\cdots$	$\cdots$	$\cdots$
$\Lambda_c^+\Lambda_c^-$	0.75	0.62	0.39	0.75	0.62	0.40
$\Sigma_c\bar{\Sigma}_c$	0.85	0.65	0.42	0.85	0.66	0.41
$\Sigma_c^*\bar{\Sigma}_c^*$	0.88	0.70	0.50	$\cdots$	$\cdots$	$\cdots$
$\Xi_c\bar{\Xi}_c$	0.75	0.61	0.39	$\cdots$	$\cdots$	$\cdots$
$\Xi_c^*\bar{\Xi}_c^*$	0.81	0.62	0.40	0.83	0.62	0.40
$\Lambda_b^+\Lambda_b^-$	0.75	0.61	0.38	0.75	0.61	0.38
$\Sigma_b\bar{\Sigma}_b$	0.83	0.64	0.38	0.83	0.64	0.38
$\Sigma_b^*\bar{\Sigma}_b^*$	0.86	0.67	0.38	0.87	0.68	0.39
$\Xi_b\bar{\Xi}_b$	0.75	0.61	0.38	0.75	0.60	0.39
$\Xi_b^*\bar{\Xi}_b^*$	0.80	0.61	0.38	0.82	0.61	0.38

The chromomagnetic interaction V^{CM} in OGE as a unique binding mechanism was applied to study multiquark systems [35–37], such as the well-known H particle [35]:

$$V^{CM} = -\pi\alpha_s \sum_{i>j}^{6} \frac{\delta(\mathbf{r}_{ij})\boldsymbol{\sigma}_i \cdot \boldsymbol{\sigma}_j \boldsymbol{\lambda}_i \cdot \boldsymbol{\lambda}_j}{6m_i m_j}. \tag{30}$$

It gives a strong attraction in the formation of the multiquark states. However, some research of multiquark states indicates that the chromomagnetic interaction as a unique binding mechanism has encountered some difficulties [38]. The contributions of the chromomagnetic interaction in all possible $B\bar{B}$ bound states in Table III are listed in Table V. It can be seen that the chromomagnetic interaction provides a strong attraction in the low-spin $B\bar{B}$ bound states, such as the states $\Lambda\bar{\Lambda}$, $\Lambda_c\bar{\Lambda}_c$, and $\Lambda_b\bar{\Lambda}_b$. This is another reason why the low-spin $B\bar{B}$ states can form compact bound states $q^3\bar{q}^3$ in the color flux-tube model. The chromomagnetic interaction in a bound state containing a baryon and an antibaryon with $S = \frac{1}{2}$ is stronger than that in a bound state containing a baryon and an antibaryon with $S = \frac{3}{2}$ (see Table V), such as $\Sigma\bar{\Sigma}$ and $\Sigma^*\bar{\Sigma}^*$, $\Sigma_c\bar{\Sigma}_c$ and $\Sigma_c^*\bar{\Sigma}_c^*$, $\Sigma_b\bar{\Sigma}_b$ and $\Sigma_b^*\bar{\Sigma}_b^*$, and so on. Our conclusions are qualitatively consistent with the conclusions of the study of the spectroscopy of hexaquark states $q^3\bar{q}^3$ [37].

TABLE V. The contributions of the chromomagnetic interaction in all possible $B\bar{B}$ bound states listed in Table III, units in MeV.

States	0^{-+}	1^{--}	States	0^{-+}	1^{--}
$N\bar{N}$	-642	$\cdots$	$\Sigma_c\bar{\Sigma}_c$	-304	-296
$\Lambda\bar{\Lambda}$	-826	-813	$\Sigma_c^*\bar{\Sigma}_c^*$	-72	$\cdots$
$\Sigma\bar{\Sigma}$	-319	$\cdots$	$\Xi_c\bar{\Xi}_c$	-407	$\cdots$
$\Xi\bar{\Xi}$	-384	$\cdots$	$\Xi_c^*\bar{\Xi}_c^*$	-249	-180
$\Delta\bar{\Delta}$	-115	$\cdots$	$\Lambda_b^+\Lambda_b^-$	-840	-839
$\Sigma^*\bar{\Sigma}^*$	-118	$\cdots$	$\Sigma_b\bar{\Sigma}_b$	-315	-314
$\Xi^*\bar{\Xi}^*$	-200	-134	$\Sigma_b^*\bar{\Sigma}_b^*$	-83	-32
$\Omega^-\Omega^+$	-154	$\cdots$	$\Xi_b\bar{\Xi}_b$	-468	-189
$\Lambda_c^+\Lambda_c^-$	-826	-814	$\Xi_b^*\bar{\Xi}_b^*$	-267	-196

For the light nonstrange hexaquark system $nnn\bar{n}\,\bar{n}\,\bar{n}$, there are two interesting states, $N\bar{N}$ and $\Delta\bar{\Delta}$ with $J^{PC} = 0^{-+}$. The masses are 1832 MeV and 2384 MeV, respectively, which are very close to the experimental data of the $X(1835)$ and $X(2370)$ observed in the radiative decay of J/ψ by the BES Collaboration. Therefore, the bound states $N\bar{N}$ and $\Delta\bar{\Delta}$ may be the dominant components of the $X(1835)$ and $X(2370)$, respectively. Our interpretation is consistent with many authors' points of view with different models [8]. Alternatively, the $X(2370)$ could also be explained as the bound state $N(1440)\bar{N}$ or $N\bar{N}(1440)$ in the Bethe-Salpeter equation approach [39]. For the light strange hexaquark systems $nns\bar{n}\,\bar{n}\,\bar{s}$ and $nss\bar{n}\,\bar{s}\,\bar{s}$, several weakly bound states, $\Lambda\bar{\Lambda}$, $\Sigma\bar{\Sigma}$, $\Sigma^*\bar{\Sigma}^*$, $\Xi\bar{\Xi}$, and $\Xi^*\bar{\Xi}^*$, can exist in the color flux-tube model. The mass of the bound state $\Lambda\bar{\Lambda}$ with $J^{PC} = 1^{--}$, 2186 MeV, is close to the experimental value of the $Y(2175)$. Therefore, the dominant component of $Y(2175)$ could be treated as a bound state $\Lambda\bar{\Lambda}$ in our model. The interpretation of $Y(2175)$ as the bound state $\Lambda\bar{\Lambda}$ with $J^{PC} = 1^{--}$ is also proposed in other constituent quark models [10,40]. The weakly bound state of $\Sigma\bar{\Sigma}$ was also obtained in Ref. [40]. The states $\Lambda\bar{\Lambda}$, $\Sigma\bar{\Sigma}$, and $\Xi\bar{\Xi}$ were investigated in the framework of the Bethe-Salpeter equation with a phenomenological potential, and similar conclusions were arrived at [39].

For the heavy hexaquark systems with a $c\bar{c}$ or $b\bar{b}$ pair, the states $\Lambda_c^+\Lambda_c^-$, $\Sigma_c\bar{\Sigma}_c$, $\Xi_c\bar{\Xi}_c$, $\Xi_c^*\bar{\Xi}_c^*$, $\Lambda_b^+\Lambda_b^-$, $\Sigma_b\bar{\Sigma}_b$, and $\Xi_b\bar{\Xi}_b$ can form bound states with large binding energies, while the binding energies of states $\Sigma_c^*\bar{\Sigma}_c^*$ and $\Sigma_b^*\bar{\Sigma}_b^*$ are tens of MeV. Concerning the states $\Omega^-\Omega^+$, $\Omega_c^0\bar{\Omega}_c^0$, $\Omega_c^{0*}\bar{\Omega}_c^{0*}$, and $\Omega_b^-\Omega_b^+$, only the state $\Omega^-\Omega^+$ has a shallow bound state with binding energy about 8 MeV; the others are unbound. Compared with the state $\Omega\bar{\Omega}$, the states $\Omega_c^0\bar{\Omega}_c^0$, $\Omega_c^{0*}\bar{\Omega}_c^{0*}$, and $\Omega_b^-\Omega_b^+$ have a bigger quark mass—although it makes the kinetic energies lower, it also reduces the chromomagnetic interaction, which does not favor forming a bound state in the model. The heavy baryonia with a $c\bar{c}$ pair were systematically investigated within the framework of the OBE (π, η, ρ, ω, ϕ, and σ) model, and it is suggested that the states $\Lambda_c^+\Lambda_c^-$, $\Sigma_c\bar{\Sigma}_c$, and $\Xi_c\bar{\Xi}_c$ have deep attractive potentials in the short-distance domain [41], which is qualitatively consistent with our conclusions. It seems that the OBE effect in the short distance can be described by the coupling of different color flux-tube structures in our model, which deserves future study. The heavy partners $\Lambda_c\bar{\Lambda}_c$ (with mass 4330 MeV) and $\Lambda_b\bar{\Lambda}_b$ (with mass 10877 MeV) of the bound states $\Lambda\bar{\Lambda}$ may be used to explain the states $Y(4260)$ or $Y(4360)$, and $Y_b(10890)$, respectively. The interpretation is consistent with Refs. [9,42].

The $B\bar{B}$ bound states, if they really exist, can be observed in the corresponding $B\bar{B}$ invariant mass spectrum when they are produced in the e^+e^- annihilation and charmonium or bottomonium decay processes; they can eventually decay into three color-singlet mesons. Before the occurrence of this decay, the hidden-color hexaquark states must change into several colorless subsystems by means of the breakdown and recombination of color flux tubes because of a color confinement. This decay mechanism is similar to compound nucleus formation, and therefore should induce a resonance, which is called a "color-confined, multiquark resonance state" in the color flux-tube model [43]. It is different from all of those microscopic resonances discussed by S. Weinberg [44].

V. SUMMARY

The mass spectrum of $B\bar{B}$ states containing u, d, s, c, and b quarks has been studied in the color flux-tube model with a multibody confinement interaction. A powerful numerical method with high precision, GEM, is used in the calculation. The numerical results indicate that many low-spin $B\bar{B}$ states can form compact hexaquark states $q^3\bar{q}^3$ which do not directly decay into a baryon and an antibaryon but into three color-singlet mesons by means of the breakdown and recombination of color flux tubes, while the high-spin $B\bar{B}$ states cannot form bound states. The multibody confinement interaction as a binding mechanism can globally give more attractions in the short-distance domain than the two-body one does in the study of the multiquark calculations; the effect seems to be equivalent to that of the ω and ρ meson exchanges. In addition, the chromomagnetic interaction can provide a strong attraction for the low-spin states.

The $B\bar{B}$ bound states, $\Sigma\bar{\Sigma}$, $\Sigma^*\bar{\Sigma}^*$, $\Xi\bar{\Xi}$, $\Xi^*\bar{\Xi}^*$, $\Sigma_c\bar{\Sigma}_c$, $\Xi_c\bar{\Xi}_c$, $\Xi_c^*\bar{\Xi}_c^*$, $\Sigma_b\bar{\Sigma}_b$, and $\Xi_b\bar{\Xi}_b$, predicted by the color flux-tube model, if they really exist, can be observed in the corresponding $B\bar{B}$ invariant mass spectrum when they are produced in the e^+e^- annihilation and charmonium or bottomonium decay processes. The dominant components of the new hadron states, $X(1835)$, $X(2370)$, $Y(2175)$, $Y(4260)$, and $Y_b(10890)$, may be interpreted as $N\bar{N}$, $\Delta\bar{\Delta}$,

$\Lambda\bar{\Lambda}$, $\Lambda_c\bar{\Lambda}_c$, and $\Lambda_b\bar{\Lambda}_b$ compact bound states, respectively. To justify this, the calculation of the decay properties of these states is critical. However, the present difficulty lies in the lack of reliable knowledge of the breakdown and recombination of color flux tubes, which is worth studying in the future.

ACKNOWLEDGMENTS

This research is partly supported by the National Science Foundation of China under Contracts No. 11305274, No. 11047140, No. 11175088, No. 11035006, and No. 11265017, and by the Chongqing Natural Science Foundation under Project No. cstc2013jcyjA00014.

[1] E. Fermi and C. N. Yang, Phys. Rev. **76**, 1739 (1949).
[2] S. Sakata, Prog. Theor. Phys. **16**, 686 (1956).
[3] A. S. Goldhaber and M. Goldhaber, Phys. Rev. Lett. **34**, 36 (1975); C. B. Dover, S. H. Kahana, and T. L. Trueman, Phys. Rev. D **16**, 799 (1977); C. B. Dover and M. Goldhaber, Phys. Rev. D **15**, 1997 (1977); G. C. Rossi and G. Veneziano, Nucl. Phys. **B123**, 507 (1977); I. S. Shapiro, Phys. Rep. **35**, 129 (1978); L. Montanet, G. C. Rossi, and G. Veneziano, Phys. Rep. **63**, 151 (1980).
[4] K. Abe *et al.* (Belle Collaboration), Phys. Rev. Lett. **88**, 181803 (2002); J. Z. Bai *et al.* (BES Collaboration), Phys. Rev. Lett. **91**, 022001 (2003); M. Ablikim *et al.* (BES Collaboration), Phys. Rev. Lett. **95**, 262001 (2005); Phys. Rev. D **71**, 072006 (2005); Phys. Rev. Lett. **106**, 072002 (2011).
[5] Y. J. Lee *et al.* (Belle Collaboration), Phys. Rev. Lett. **93**, 211801 (2004); B. Aubert *et al.* (*BABAR* Collaboration), Phys. Rev. D **76**, 092006 (2007).
[6] G. Pakhlova *et al.* (Belle Collaboration), Phys. Rev. Lett. **101**, 172001 (2008).
[7] N. Brambilla *et al.*, Eur. Phys. J. C **71**, 1534 (2011) and references therein.
[8] C. S. Gao and S. L. Zhu, Commun. Theor Phys. **42**, 844 (2004); A. Datta and P. J. O'Donnell, Phys. Lett. B **567**, 273 (2003); G. J. Ding and M. L. Yan, Phys. Rev. C **72**, 015208 (2005); Eur. Phys. J. A **28**, 351 (2006); C. Liu, Eur. Phys. J. C **53**, 413 (2008).
[9] C. F. Qiao, Phys. Lett. B **639**, 263 (2006); J. Phys. G **35**, 075008 (2008).
[10] L. Zhao, N. Li, S. L. Zhu, and B. S. Zou, Phys. Rev. D **87**, 054034 (2013).
[11] C. R. Deng, J. L. Ping, Y. C. Yang, and F. Wang, Phys. Rev. D **86**, 014008 (2012).
[12] S. Godfrey and J. Napolitano, Rev. Mod. Phys. **71**, 1411 (1999).
[13] N. Isgur and G. Karl, Phys. Rev. D **18**, 4187 (1978); **19**, 2653 (1979); **20**, 1191 (1979).
[14] Y. Fujiwara, C. Nakamoto, and Y. Suzuki, Phys. Rev. C **54**, 2180 (1996); Y. Fujiwara, M. Kohno, C. Nakamoto, and Y. Suzuki, Phys. Rev. C **64**, 054001 (2001); Y. Fujiwara, K. Miyagawa, M. Kohno, Y. Suzuki, and C. Nakamoto, Nucl. Phys. **A737**, 243 (2004).
[15] C. R. Deng, J. L. Ping, P. Zhou, and F. Wang, Chinese Phys. C **37**, 033101 (2013).
[16] C. R. Deng, J. L. Ping, H. Wang, P. Zhou, and F. Wang, Phys. Rev. D **86**, 114035 (2012).
[17] C. R. Deng, J. L. Ping, F. Wang, and T. Goldman, Phys. Rev. D **82**, 074001 (2010).
[18] J. L. Ping, C. R. Deng, F. Wang, and T. Goldman, Phys. Lett. B **659**, 607 (2008).
[19] F. Wang and C. W. Wong, Nuovo Cimento A **86**, 283 (1985).
[20] H. X. Huang, P. Xu, J. L. Ping, and F. Wang, Phys. Rev. C **84**, 064001 (2011).
[21] C. Alexandrou, P. de Forcrand, and A. Tsapalis, Phys. Rev. D **65**, 054503 (2002); T. T. Takahashi, H. Suganuma, Y. Nemoto, and H. Matsufuru, Phys. Rev. D **65**, 114509 (2002); F. Okiharu, H. Suganuma, and T. T. Takahashi, Phys. Rev. D **72**, 014505 (2005); Phys. Rev. Lett. **94**, 192001 (2005).
[22] T. Goldman and S. Yankielowicz, Phys. Rev. D **12**, 2910 (1975).
[23] N. Isgur and J. Paton, Phys. Rev. D **31**, 2910 (1985).
[24] F. Bissey, F.-G. Cao, A. Kitson, A. Signal, D. Leinweber, B. Lasscock, and A. Williams, Phys. Rev. D **76**, 114512 (2007).
[25] R. L. Jaffe and F. Wilczek, Phys. Rev. Lett. **91**, 232003 (2003); M. Karliner and H. J. Lipkin, Phys. Lett. B **575**, 249 (2003).
[26] G. S. Bali, Phys. Rev. D **62**, 114503 (2000); C. Semay, Eur. Phys. J. A **22**, 353 (2004); N. Cardoso, M. Cardoso, and P. Bicudo, Phys. Lett. B **710**, 343 (2012).
[27] E. Klempt and J. M. Richard, Rev. Mod. Phys. **82**, 1095 (2010).
[28] J. Vijande, F. Fernandez, and A. Valcarce, J. Phys. G **31**, 481 (2005).
[29] J. Weinstein and N. Isgur, Phys. Rev. D **27**, 588 (1983).
[30] E. Hiyama, Y. Kino, and M. Kamimura, Prog. Part. Nucl. Phys. **51**, 223 (2003).
[31] Y. C. Yang, C. R. Deng, J. L. Ping, and T. Goldman, Phys. Rev. D **80**, 114023 (2009).
[32] D. R. Entem and F. Fernandez, Phys. Rev. C **73**, 045214 (2006).
[33] H. X. Huang, H. R. Pang, and J. L. Ping, Mod. Phys. Lett. A **26**, 1231 (2011).
[34] J. Vijande, A. Valcarce, and J. M. Richard, Phys. Rev. D **85**, 014019 (2012); J. M. Richard, Phys. Rev. C **81**, 015205 (2010); J. Vijande, A. Valcarce, and J. M. Richard, Phys. Rev. D **76**, 114013 (2007).
[35] R. L. Jaffe, Phys. Rev. Lett. **38**, 195 (1977).
[36] B. Silvestre-Brac, Phys. Rev. D **46**, 2179 (1992); B. Silvestre-Brac and J. Leandri, Phys. Rev. D **45**, 4221 (1992).

[37] G. J. Ding, J. L. Ping, and M. L. Yan, Phys. Rev. D **74**, 014029 (2006).
[38] J. L. Rosner, Phys. Rev. D **33**, 2043 (1986); G. Karl and P. Zenczykowski, Phys. Rev. D **36**, 2079 (1987); **36**, 3520 (1987).
[39] Z. G. Wang, Eur. Phys. J. A **47**, 71 (2011).
[40] M. Abud, F. Buccella, and F. Tramontano, Phys. Rev. D **81**, 074018 (2010).
[41] N. Lee, Z. G. Luo, X. L. Chen, and S. L. Zhu, Phys. Rev. D **84**, 014031 (2011).
[42] Y. D. Chen and C. F Qiao, Phys. Rev. D **85**, 034034 (2012).
[43] F. Wang, J. L. Ping, H. R. Pang, and L. Z. Chen, Nucl. Phys. **A790**, 493c (2007).
[44] S. Weinberg, *The Quantum Theory of Fields* (Cambridge University Press, Cambridge, England, 1995), Vol. 1, p. 159.